Intramolecular Hydroamination Catalyzed by Cationic Rhodium and Iridium Complexes with Bidentate Nitrogen-Donor Ligands

Suzanne Burling,[†] Leslie D. Field,*[,†] Barbara A. Messerle,*[,‡] and Peter Turner[†]

School of Chemistry, University of Sydney, Sydney, NSW 2006, Australia, and School of Chemistry, University of New South Wales, Sydney, NSW 2052, Australia

Received December 18, 2003

Cationic rhodium(I) and iridium(I) complexes of the general formula $[M(N-N)(CO)_2]^+[X]^-$, incorporating the bidentate heterocyclic nitrogen donor ligands (N−N) bis(1-methylimidazol-2-yl)methane (bim) and bis(1-pyrazolyl)methane (bpm), are efficient catalysts for hydroamination. The cyclization of an aliphatic aminoalkyne to the corresponding five-membered imine heterocycle was achieved in good yield with excellent regioselectivity using both rhodium and iridium catalysts. The nature of the counterion to the cationic catalysts has a significant effect on the rate of the hydroamination reaction and interionic contacts between the metal complexes and their counterions in solution were clearly visible by NMR spectroscopy using the nuclear Overhauser effect, indicating a strong anion/cation interaction in solution. The nature of the coligands also had a significant effect on the efficiency of the metal complexes as catalysts, and complexes containing phosphine coligands were less effective catalysts compared to those complexes containing CO coligands. The X-ray crystal structure of the new iridium(I) complex $[Ir(bim)(CO)_2]^+[BPh_4]^-$ (**2**) is reported, as well as the synthesis and characterization of the Rh complex $[Rh(bpm)(CO)_2]^+[BPh_4]^-$ (**3**).

Introduction

The hydroamination reaction involves the addition of N−H bonds across carbon−carbon double and triple bonds and offers an atom-efficient pathway to produce new primary, secondary, and tertiary amines as well as imines and enamines.[1,2] The syntheses of amines, enamines, and imines are key reactions in organic chemistry and in the production of chemicals on an industrial scale.[3] While the hydroamination reaction is thermodynamically reasonable, there is a high activation barrier under normal conditions, necessitating the use of a catalyst.[1−3] A number of catalysts which effect hydroamination have been developed,[2,4] and examples of catalysts which have been successful for intramolecular hydroamination reactions include both late-transition-metal[1,5] and lanthanide complexes.[6] The area of intermolecular hydroamination has provided a greater challenge, and recently significant developments in active group 4 metal complexes, including alkyltitanocenes and titanium amido complexes, have been made, in particular with titanium complexes with labile nitrogen donor ligands.[7] Titanium complexes are, however, extremely oxophilic, and this reduces their functional group tolerance. While the lanthanide catalysts are very efficient catalysts for intermolecular hydroamination, their sensitivity to oxygen and moisture have limited their general use in many applications.[2] The late-transition-metal catalysts for hydroamination generally have greater functional group tolerance and lower oxygen and moisture sensitivity. There are now several reports of catalytic systems of intermolecular hydroamination using rhodium[8] and iridium[9] complexes.

We recently reported the successful application of the cationic rhodium(I) bis(1-methylimidazol-2-yl)methane

[†] University of Sydney.
[‡] University of New South Wales.

(1) See for example: Müller, T. E.; Beller, M. *Chem. Rev.* **1998**, *98*, 675.
(2) Pohlki, F.; Doye, S. *Chem. Soc. Rev.* **2003**, *32*, 104.
(3) Taube, R. In *Applied Homogeneous Catalysis with Organometallic Compounds*;=, 1st ed.; Cornils, B., Herrmann, W. A., Eds.; VCH: Weinheim, Germany, 1996; Vol. 1, p 507.
(4) Nobis, M.; Driessen-Hölscher, B. *Angew. Chem., Int. Ed.* **2001**, *40*, 3983.
(5) Hegedus, L. S.; McKearin, J. M. *J. Am. Chem. Soc.* **1982**, *104*, 2444. Tamaru, Y.; Hojo, M.; Higashimura, H.; Yoshida, Z. *J. Am. Chem. Soc.* **1988**, *110*, 3994. McGrane, P. L.; Livinghouse, T. *J. Am. Chem. Soc.* **1993**, *115*, 11485. Müller, T. E. *Tetrahedron Lett.* **1998**, *39*, 5961. Müller, T. E.; Pleier, A.-K. *J. Chem. Soc., Dalton Trans.* **1999**, 583. Kadota, I.; Shibuya, A.; Lutete, L. M.; Yamamoto, Y. *J. Org. Chem.* **1999**, *64*, 4570. Müller, T. E.; Grosche, M.; Herdtweck, E.; Pleier, A.-K.; Walter, E.; Yan, Y.-K. *Organometallics* **2000**, *19*, 170. Kondo, T.; Okada, T.; Suzuki, T.; Mitsudo, T. *J. Organomet. Chem.* **2001**, *622*, 149. Shimada, T.; Yamamoto, Y. *J. Am. Chem. Soc.* **2002**, *124*, 12670. Togni, A.; Fadini, L. *Chem. Commun.* **2003**, 30.
(6) Li, Y.; Marks, T. J. *J. Am. Chem. Soc.* **1996**, *118*, 9295. Arredondo, V. M.; McDonald, F. E.; Marks, T. J. *J. Am. Chem. Soc.* **1998**, *120*, 4871. Giardello, M. A.; Conticello, V. P.; Brard, L.; Gagne, M. R.; Marks, T. J. *J. Am. Chem. Soc.* **1994**, *116*, 10241. Gagne, M. R.; Stern, C. L.; Marks, T. J. *J. Am. Chem. Soc.* **1992**, *114*, 275. Gagne, M. R.; Brard, L.; Conticello, V. P.; Giardello, M. A.; Stern, C. L.; Marks, T. J. *Organometallics* **1992**, *11*, 2003. Arredondo, V. M.; McDonald, F. E.; Marks, T. J. *Organometallics* **1999**, *18*, 1949. Ryu, J.-S.; McDonald, F. E.; Marks, T. J. *Org. Lett.* **2001**, *3*, 3091. Douglass, M. R.; Ogasawara, M.; Hong, S.; Metz, M. V.; Marks, T. J. *Organometallics* **2002**, *21*, 283. Kim, Y. K.; Livinghouse, T.; Horino, Y. *J. Am. Chem. Soc.* **2003**, *125*, 9560.
(7) Haak, E.; Bytschkov, I.; Doye, S. *Angew. Chem., Int. Ed.* **1999**, *38*, 3389. Haak, E.; Siebeneicher, H.; Doye, S. *Org. Lett.* **2000**, *2*, 1935. Pohlki, F.; Doye, S. *Angew. Chem., Int. Ed.* **2001**, *40*, 2305. Cao, C.; Ciszewski, J. T.; Odom, A. L. *Organometallics* **2001**, *20*, 5011. Bytschkov, I.; Doye, S. *Tetrahedron Lett.* **2002**, *43*, 3715. Tillack, A.; Castro, I. G.; Hartung, C. G.; Beller, M. *Angew. Chem., Int. Ed.* **2002**, *41*, 2541. Ackermann, L.; Bergman, R. G. *Org. Lett.* **2002**, *4*(9), 1475. Bytschkov, I.; Doye, S. *Eur. J. Org. Chem.* **2003**, 935. Shi, Y.; Hall, C.; Ciszewski, J. T.; Cao, C.; Odom, A. L. *Chem. Commun.* **2003**, 586.

10.1021/om0343871 CCC: $27.50
Publication on Web 03/11/2004

complex (**1a**) to the intramolecular hydroamination of alkynes.[10] This demonstrated that cationic, coordinatively unsaturated complexes of group 9 metals with bidentate nitrogen donors are potentially active catalysts for the hydroamination reaction. A number of charged transition-metal complexes catalyze the intramolecular hydroamination of aminoalkynes,[11] while a recently developed dicationic palladium complex has been shown to catalyze an intermolecular hydroamination reaction.[12] There is increasing evidence that, for a charged transition-metal catalyst, the activity, lifetime, stability, and product selectivity of the reaction are significantly influenced by the nature of the counterion.[13−18] Smaller, more tightly binding anions such as PF_6^-, BF_4^-, and ClO_4^- are, in some cases, less favored as counterions for many homogeneous catalysts,[13] whereas tetraphenylborate has been commonly utilized as a counterion, due to its size, its inertness, and its tendency to more readily form stable crystalline compounds. However, although BPh_4^- is usually considered as an unreactive or "innocent" counterion, it is known to act as a phenylating agent toward organic molecules and also to participate in π-interactions with metal centers.[14] The anion effect has received the most attention in studies of homogeneous olefin polymerization catalysis,[15] and some of the most extensively used anions of recent interest in olefin polymerization chemistry are the perfluorophenylborates and aluminates, including the tetrakis(3,5-bis(trifluoromethyl)phenyl)borate anion.[16] These polyfluorinated anions have properties such as low nucleophilicity, chemical inertness, improved solubility, and weaker coordinating strength,[17] all of which can enhance catalyst efficiency.

In this paper, we report the results of intramolecular hydroamination reactions of aminoalkynes to form nitrogen-containing heterocycles catalyzed by the cationic Rh(I) and Ir(I) complexes $[Rh(bim)(CO)_2]^+[X]^-$ (**1**: **a**, X = BPh_4; **b**, X = PF_6; **c**, X = BF_4), $[Rh(bim)(PPh_3)_2]^+[BPh_4]^-$ (**1d**), $[Ir(bim)(CO)_2]^+[BPh_4]^-$ (**2**), $[Rh(bpm)(CO)_2]^+[BPh_4]^-$ (**3**), and $[Ir(bpm)(CO)_2]^+[BPh_4]^-$ (**4**) with the bidentate nitrogen donor ligands bis(1-methylimidazol-2-yl)methane (bim) and bis(1-pyrazolyl)methane (bpm).

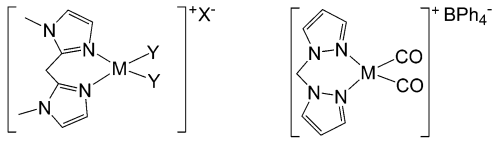

M = Rh Y = CO X = BPh_4 **1a**
M = Rh Y = CO X = PF_6 **1b**
M = Rh Y = CO X = BF_4 **1c**
M = Rh Y = PPh_3 X = BPh_4 **1d**
M = Ir Y = CO X= BPh_4 **2**

M = Rh **3**
= Ir **4**

In solution, there is a strong interaction between the cationic complex and the counterion, and both the nature of the counterion and the coligands have a significant effect on the catalytic efficiency. We also report the synthesis and characterization of the new cationic rhodium(I) complex $[Rh(bpm)(CO)_2]^+[BPh_4]^-$ (**3**) and present the crystallographic characterization of the recently reported iridium(I) complex $[Ir(bim)(CO)_2]^+[BPh_4]^-$ (**2**).[19]

Results and Discussion

Synthesis of Metal Complexes. The nitrogen donor ligands bim and bpm, used in the synthesis of complexes **1**−**4**, were prepared by previously reported methods.[10,20] The cationic dicarbonyl complexes of rhodium and iridium $[Rh(bim)(CO)_2]^+[BPh_4]^-$ (**1a**), $[Ir(bim)(CO)_2]^+[BPh_4]^-$ (**2**), $[Rh(bpm)(CO)_2]^+[BPh_4]^-$ (**3**), and $[Ir(bpm)(CO)_2]^+[BPh_4]^-$ (**4**) were prepared in good yield by addition of the bidentate ligand to the appropriate metal precursor in methanol. The complexes were precipitated as air-stable crystalline solids with tetraphenylborate counterions.

The synthesis of $[Rh(bim)(CO)_2]^+[BPh_4]^-$ (**1a**) has been reported previously,[10,21] and the synthesis of the rhodium(I) bis(1-pyrazolyl)methane complex **3** followed an analogous route. Two equivalents of the bpm ligand in methanol was added to $[Rh(CO)_2Cl]_2$ in methanol under nitrogen, and $[Rh(bpm)(CO)_2]^+[BPh_4]^-$ (**3**) was precipitated by addition of $NaBPh_4$ as a fine yellow crystalline solid. In air, the complex is stable indefinitely; however, it decomposes rapidly in solution. The synthesis of the rhodium complexes **1b**,**c** again followed a similar route, with the addition of methanol solution of the bim ligand to a solution of $[Rh(CO)_2Cl]_2$ in methanol under nitrogen, followed by addition of an excess of the appropriate counterion and isolation of the resulting precipitates. The synthesis of **1d** has been reported elsewhere.[22] The synthesis of $[Rh(bpm^*)(CO)_2]^+[BF_4]^-$ (bpm* = bis(3,5-dimethylpyrazolyl)methane) has also been reported recently.[23]

(8) Brunet, J.-J.; Neibecker, D.; Philippot, K. *Tetrahedron Lett.* **1993**, *34*, 3877. Brunet, J.-J.; Commenges, G.; Neibecker, D.; Philippot, K. *J. Organomet. Chem.* **1994**, *469*, 221. Beller, M.; Trauthwein, H.; Eichberger, M.; Breindl, C.; Herwig, J.; Müller, T. E.; Thiel, O. R. *Chem. Eur. J.* **1999**, *5*, 1306. Tillack, A.; Hartung, C. G.; Trauthwein, H.; Beller, M. *J. Org. Chem.* **2001**, *66*, 6339.

(9) Casalnuovo, A. L.; Calabrese, J. C.; Milstein, D. *J. Am. Chem. Soc.* **1988**, *110*, 6738. Dorta, R.; Egli, P.; Zurcher, F.; Togni, A. *J. Am. Chem. Soc.* **1997**, *119*, 10857.

(10) Burling, S.; Field, L. D.; Messerle, B. A. *Organometallics* **2000**, *19*, 87.

(11) Müller, T. E.; Grosche, M.; Herdtweck, E.; Pleier, A.-K.; Walter, E.; Yan, Y.-K. *Organometallics* **2000**, *19*, 170.

(12) Li, K.; Hii, K. K. *Chem. Commun.* **2003**, 1132. Li, K.; Hii, K. K.; Horton, P. N.; Hursthouse, M. B. *J. Organomet. Chem.* **2003**, *665*, 250.

(13) Strauss, S. H. *Chem. Rev.* **1993**, *93*, 927.

(14) Aresta, M.; Quaranta, E.; Tommasi, I. *New J. Chem.* **1996**, *21*, 595. Schrock, R. R.; Osborn, J. A. *Inorg. Chem.* **1970**, *9*, 2339.

(15) Yang, X.; Stern, C.; Marks, T. J. *J. Am. Chem. Soc.* **1994**, *116*, 10015. Liting, L.; Stern, C. L.; Marks, T. J. *Organometallics* **2000**, *19*, 3332. Chen, Y.-X.; Metz, M. V.; Li, L.; Stern, C. L.; Marks, T. J. *J. Am. Chem. Soc.* **1998**, *120*, 6287. Chen, Y.-X.; Stern, C. L.; Yang, S.; Marks, T. J. *J. Am. Chem. Soc.* **1996**, *118*, 12451. Chen, Y.-X.; Stern, C. L.; Marks, T. J. *J. Am. Chem. Soc.* **1997**, *119*, 2582. Jia, L.; Yang, X.; Stern, C. L.; Marks, T. J. *Organometallics* **1997**, *16*, 842.

(16) Johnson, L. K.; Mecking, S.; Brookhart, M. *J. Am. Chem. Soc.* **1996**, *118*, 267. Mecking, S.; Johnson, L. J.; Wang, L.; Brookhart, M. *J. Am. Chem. Soc.* **1998**, *120*, 888. Chen, E. Y.-X.; Marks, T. J. *Chem. Rev.* **2000**, *100*, 1391.

(17) Reed, C. A. *Acc. Chem. Res.* **1998**, *31*, 133.

(18) Macchioni, A.; Bellachioma, G.; Cardaci, G.; Travaglia, M.; Zuccaccia, C.; Milani, B.; Corso, G.; Zangrando, E.; Mestroni, G.; Carfagna, C.; Formica, M. *Organometallics* **1999**, *18*, 3061. LaPointe, R. E.; Roof, G. R.; Abboud, K. A.; Klosin, J. *J. Am. Chem. Soc.* **2000**, *122*, 9560. Piers, W. E. *Chem. Eur. J.* **1998**, *4*, 13. Beswick, C. L.; Marks, T. J. *Organometallics* **1999**, *18*, 2410. Boche, G. *Angew. Chem., Int. Ed. Engl.* **1992**, *31*, 731.

(19) Burling, S.; Field, L. D.; Messerle, B. A.; Vuong, K. Q.; Turner, P. *Dalton* **2003**, 4181.

(20) Julia, S.; Sala, P.; Mazo, J. d.; Sancho, M.; Ochoa, C.; Elguero, J.; Fayet, J.-P.; Vertut, M.-C. *J. Heterocycl. Chem.* **1982**, *19*, 1141.

(21) Elgafi, S.; Field, L. D.; Messerle, B. A.; Turner, P.; Hambley, T. W. *J. Organomet. Chem.* **1999**, *588*, 69.

(22) Elgafi, S. Ph.D. Thesis, University of Sydney, 1996.

(23) Teuma, E.; Loy, M.; Le Berre, C.; Etienne, M.; Daran, J.-C.; Kalck., P.; *Organometallics* **2003**, *22*, 5261.

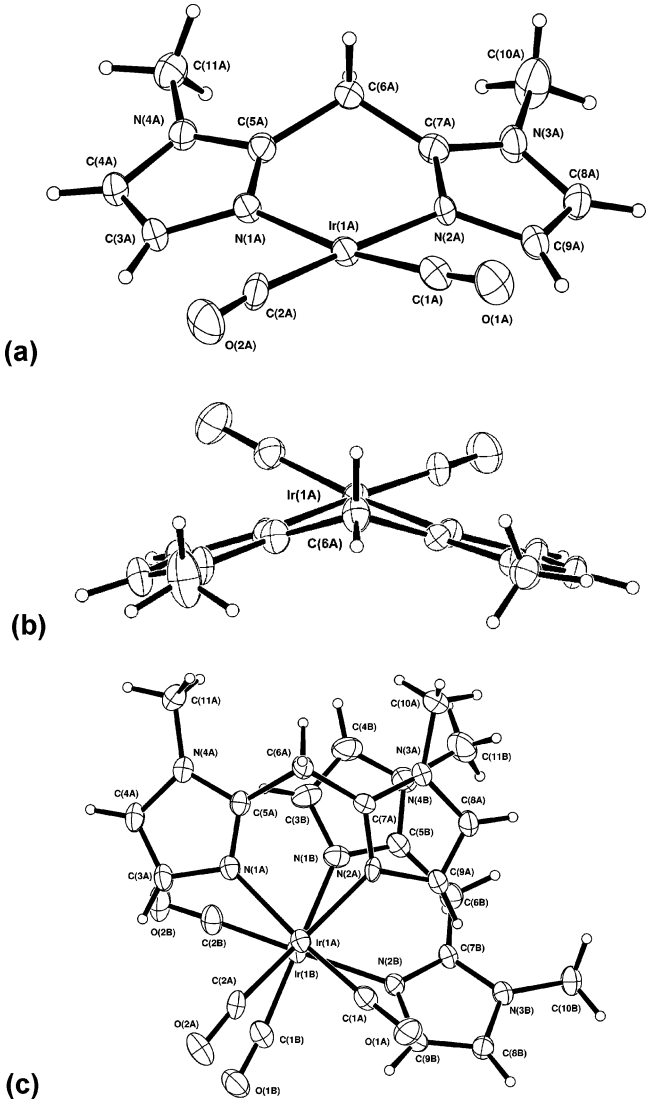

Figure 1. ORTEP[25] depictions and crystal structure numbering of the cationic fragment of $[Ir(bim)(CO)_2]^+[BPh_4]^-$ (**2**): (a) illustration of the four-coordinate square-planar geometry; (b) projection through the C6A−Ir1A axis; (c) stacking of the two independent complexes in the asymmetric unit. Displacement ellipsoids are shown at the 25% level.

The syntheses of the iridium(I) bim (**2**) and iridium(I) bpm (**4**) complexes have been reported previously.[19,24] The synthesis of **2** involved adding 2 equiv of the bim ligand to the iridium precursor $[Ir(COD)Cl]_2$ and $NaBPh_4$ and then placing the mixture under an atmosphere of carbon monoxide. $[Ir(bim)(CO)_2]^+[BPh_4]^-$ (**2**) was isolated as a fine yellow crystalline solid, which recrystallized from acetone as large red prisms suitable for X-ray diffraction analysis.

The asymmetric unit of **2** contained two crystallographically independent complex molecules and their counterions. ORTEP[25] depictions of the complexes are shown in Figure 1, and selected bond lengths and angles for the inner coordination sphere are listed in Table 1.

Complex **2** is isomorphous and isostructural with the analogous rhodium complex **1a**, published previously.[21]

(24) Field, L. D.; Messerle, B. A.; Soler, L. P.; Rehr, M.; Hambley, T. W. *Organometallics* **2003**, *22*, 2387−2395.
(25) Johnson, C. K. ORTEPII; Report ORNL-5138; Oak Ridge National Laboratory, Oak Ridge, TN, 1976.

Table 1. Selected Geometry from the Crystal Structure of $[Ir(bim)(CO)_2]^+[BPh_4]^-$ (2)

Bond Distances (Å)			
Ir(1a)−N(1a)	2.079(6)	Ir(1a)−C(1a)	1.823(8)
Ir(1a)−N(2a)	2.067(6)	Ir(1a)−C(2a)	1.836(8)
Ir(1b)−N(1b)	2.077(6)	Ir(1b)−C(1b)	1.846(8)
Ir(1b)−N(2b)	2.075(5)	Ir(1b)−C(2b)	1.843(8)
Bond Angles (deg)			
N(1a)−Ir(1a)−N(2a)	86.8(2)	N(2a)−Ir(1a)−C(1a)	90.0(3)
N(1b)−Ir(1b)−N(2b)	87.3(2)	N(2b)−Ir(1b)−C(1b)	92.3(3)
N(1a)−Ir(1a)−C(2a)	92.8(3)	C(1a)−Ir(1a)−C(2a)	90.6(3)

Table 2. Crystallographic Data for the Structure Determination of $[Ir(bim)(CO)_2]^+[BPh_4]^-$ (2)

formula	$C_{36.5}H_{35}BIrN_4O_{2.50}$
formula wt	772.70
cryst syst	monoclinic
color, habit	red, prism
space group	$P2_1/c$ (No. 14)
a	22.140(3) Å
b	11.3650(14) Å
c	28.0281(10) Å
β	111.781(7)°
V	6548.9(12) Å^3
Z	8
D_{calcd}	1.567 g cm^{-3}
$2\theta_{max}$	135.00°
hkl range	0−26, 0−13, −33 to +31
no. of rflns measd (N)	12 066
no. of unique rflns (N_0)	11 744 (R_{merge} = 0.0515)
λ(Cu Kα)	1.541 78 Å
μ(Cu Kα)	8.209 mm^{-1}
$T(\psi$ scans)$_{min,max}$	0.795, 1.000
R1(F)[a]	0.0401
wR2(F^2)[a]	0.1228
residual extrema	−1.674, 1.226 e Å^{-3}

[a] $R1 = \sum||F_o| - |F_c||/\sum|F_o|$ for $F_o > 2\sigma(F_o)$; $wR2 = (\sum w(F_o^2 - F_c^2)^2/\sum(wF_c^2)^2)^{1/2}$. For all reflections $w = 1/(\sigma^2(F_o^2) + (0.0508P)^2 + 1.8264P)$, where $P = (F_o^2 + 2F_c^2)/3$.

The geometry is essentially square planar about the iridium center, with the coordinating ligands comprising two carbonyl ligands and one bis(1-methylimidazol-2-yl)methane ligand, which provides two nitrogen donor atoms. There is a slight deviation from the ideal square-planar geometry, resulting from the small restraint placed on the heterocyclic donors by the flexible methylene bridge of the bidentate ligand. This is evident by the placement of C(6a) 1.05(1) Å out of the least-squares plane defined by C(1a)−C(2a)−N(1a)−N(2a).

The two iridium complexes in the asymmetric unit have a stacking interaction (Figure 1c), similar to that reported for the analogous rhodium complex.[21] The tendency for stacking in the solid state has been attributed to an interaction between the imidazole residues of the two independent complexes rather than by association with the phenyl rings of the tetraphenylborate counterion, which are situated far from the iridium metal center. The close contact between the two complexes is supported by the interatomic distance of 3.49(1) Å between N(1b) and the imidazole ring of complex A containing N(2a)−C(7a)−N(3a)−C(8a)−C(9a).

Interionic Contacts in Solution. Intermolecular proton−proton or proton−fluorine NOESY cross-peaks due to interactions between protons of the bim and bpm ligands and protons and fluorine atoms of the anion were observed in the NOESY (or HOESY) NMR spectra for the complexes $[Rh(bim)(CO)_2]^+[X]^-$ (**1**: **a**, X = BPh_4;

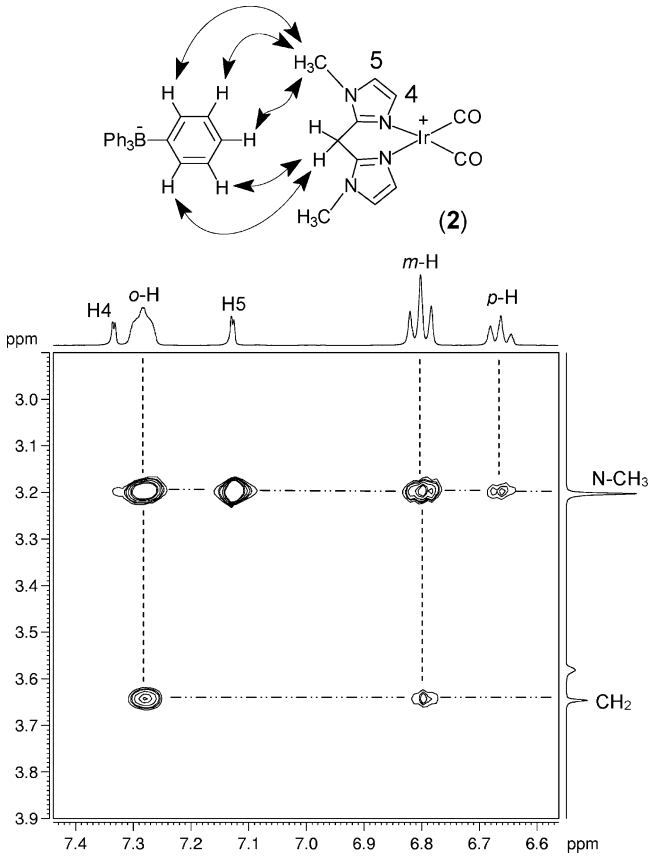

Figure 2. Interionic NOESY contacts observed for $[Ir(bim)(CO)_2]^+[BPh_4]^-$ (**2**): cross-peak region of the ^1H NOESY NMR spectrum of $[Ir(bim)(CO)_2]^+[BPh_4]^-$ (**2**) in tetrahydrofuran-d_8 at 300 K, indicating the interionic contacts between the ortho, meta, and para protons of BPh_4^- and the *N*-CH_3 and CH_2 protons of the ligand.

b,X=PF_6),$[Ir(bim)(CO)_2]^+[BPh_4]^-$(**2**),$[Rh(bpm)(CO)_2]^+[BPh_4]^-$ (**3**), and $[Ir(bpm)(CO)_2]^+[BPh_4]^-$ (**4**) in solution.

For the complexes $[Rh(bim)(CO)_2]^+[BPh_4]^-$ (**1a**) and $[Ir(bim)(CO)_2]^+[BPh_4]^-$ (**2**), strong proton−proton NOESY cross-peaks were observed between protons of the bidentate nitrogen donor ligand and the protons of the tetraphenylborate counterion (Figure 2). Clear, strong NOE interactions were evident between the ortho and para hydrogen atoms of the BPh_4^- anion and the *N*-Me and bridging methylene group of the bis(1-methylimidazol-2-yl)methane ligand in complexes **1** and **2** (see Figure 2). No intermolecular contacts were observed between the imidazole protons H4 and H5 and the counterions. The region of the NOESY spectrum of $[Ir(bim)(CO)_2]^+[BPh_4]^-$ (**2**) shown in Figure 2 illustrates the relative strengths of the interionic interactions. Only one set of phenyl resonances is observed for BPh_4^-, and this indicates that there is rapid internal motion in the anion. However, the interaction between the anion and cation is sufficiently long-lived to permit the buildup of strong NOE interactions. This is a dynamic system, and it is difficult to quantify the NOE interactions; however, the strongest interactions between the cationic complex and the counterion are at the edge of the metal complex at the periphery of the ligand structure, away from the metal center.

Intermolecular contacts have been previously reported for metal complexes coordinating the bis(1-pyrazolyl)methane ligand.[26,27] In particular, interionic contacts have been previously identified for the analogous iridium complex $[Ir(bpm)(CO)_2]^+[BPh_4]^-$ (**4**), where interactions were observed between H3 and H4 of the pyrazole ring and the meta and para protons of tetraphenylborate,[27] and the bridging methylene group also produced interionic contacts with the anion.

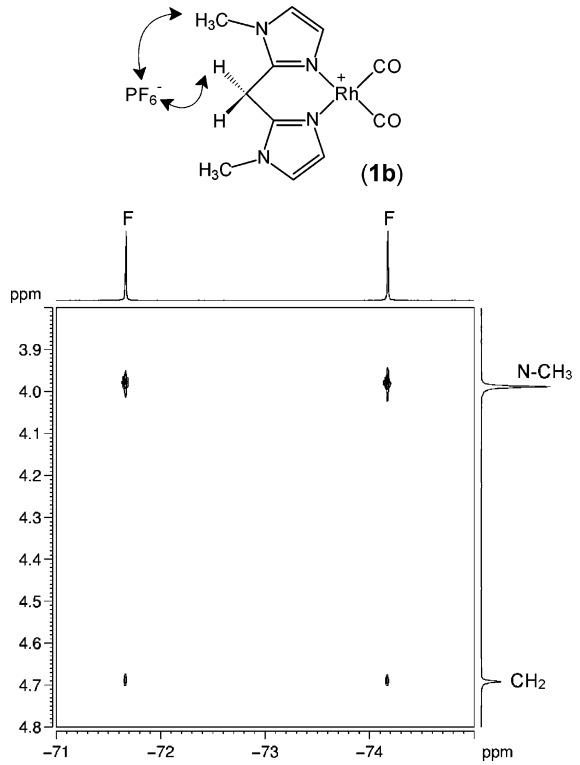

Figure 3. Section of the $^{19}F\{^1H\}$ HOESY NMR spectrum of $[Rh(bim)(CO)_2]^+[PF_6]^-$ (**1b**) in acetone-d_6, demonstrating the intermolecular HOE interactions between the rhodium cation and the hexafluorophosphate anion. The fluorine signal appears as a doublet, due to coupling to the central phosphorus atom.

Using HOESY (the heteronuclear analogue of the NOESY experiment), interionic contacts were also detected for $[Rh(bim)(CO)_2]^+[PF_6]^-$ (**1b**) in acetone-d_6 solution. In $^{19}F/^1H$ HOESY NMR experiments, HOE interactions between the protons of *N*-Me and the methylene bridge of the bis(1-methylimidazol-2-yl)-methane ligand and the fluorines of the hexafluorophosphate anion were evident (Figure 3), with no interactions between protons H4 and H5 of the imidazole ring and the fluorines of the PF_6^- counterion. This again shows that the main interaction with the counterion is not close to the metal center but, rather, away from the metal center near the remote edge of the coordinated bim ligand of the complex. The interaction predominantly at this part of the molecule could, in part, be due to a hydrogen bonding interaction between the relatively acidic methylene protons on the coordinated bim ligand and the counterion. Macchioni and co-

(26) Bellachioma, G.; Cardaci, G.; Macchioni, A.; Reichenbach, G.; Terenzi, S. *Organometallics* **1996**, *15*, 4349. Macchioni, A.; Bellachioma, G.; Cardaci, G.; Gramlich, V.; Ruegger, H.; Terenzi, S.; Venanzi, L. *Organometallics* **1997**, *16*, 2139. Macchioni, A.; Bellachioma, G.; Cardaci, G.; Cruciani, G.; Foresti, E.; Sabatino, P.; Zuccaccia, C. *Organometallics* **1998**, *17*, 5549. Zuccaccia, C.; Bellachioma, G.; Cardaci, G.; Macchioni, A. *Organometallics* **1999**, *18*, 1.
(27) Soler, L. P. Ph.D. Thesis, University of Sydney, 1999.

Table 3. Relative Efficiency of Catalysts for the Cyclization of 4-Pentyn-1-amine to 2-Methyl-1-pyrroline (thf-d_8, 1.5 mol % Catalyst)[a]

		time (h)		
complex	N_t[b]	50% conversn	98% conversn[c]	temp
$[Rh(bim)(CO)_2]^+[BPh_4]^-$ (**1a**)	17	2.0	14	60 °C
			4.5 (75)	reflux
$[Ir(bim)(CO)_2]^+[BPh_4]^-$ (**2**)	5	6.3	24 (92)	60 °C
			4.5	reflux
$[Rh(bpm)(CO)_2]^+[BPh_4]^-$ (**3**)	20	1.7	12 (90)	60 °C
			4	reflux
$[Ir(bpm)(CO)_2]^+[BPh_4]^-$ (**4**)	50	0.70	2.2	60 °C
			0.5	reflux

[a] Conditions: in thf-d_8; 1.5 mol % catalyst. [b] Turnover number = (mol of product produced)/((mol of catalyst used) h), typically calculated at time of 50% conversion. [c] Values in parentheses are the conversions (%) at the time indicated.

Scheme 1

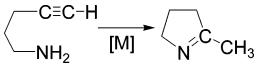

workers used $^{19}F/^1H$ HOESY NMR spectroscopy to study the interaction of the tetrafluoroborate anion with platinum complexes coordinating *N*,*N*-diimine ligands, $[Pt(Me)(\eta^2\text{-olefin})(N,N)]^+[BF_4]^-$.[28] In that work, the counterion was reported to prefer the diimine side of the complex, rather than the less hindered olefin side, and this was attributed to the expected delocalization of the positive charge on the bidentate ligand.

Catalysis: Intramolecular Hydroamination. The catalytic activity of $[Rh(bim)(CO)_2]^+[BPh_4]^-$ (**1a**) for the intramolecular hydroamination of aminoalkynes to produce nitrogen-containing heterocycles, including indoles, has already been reported.[10] Rhodium(I) and iridium(I) complexes with bim and bpm as ligands, $[Rh(bim)(CO)_2]^+[BPh_4]^-$ (**1a**), $[Ir(bim)(CO)_2]^+[BPh_4]^-$ (**2**), $[Rh(bpm)(CO)_2]^+[BPh_4]^-$ (**3**), and $[Ir(bpm)(CO)_2]^+[BPh_4]^-$ (**4**), were tested as catalysts for a standard intramolecular hydroamination using the substrate 4-pentyn-1-amine to form 2-methyl-1-pyrroline (Scheme 1, Table 3).

In the first instance, 4-pentyn-1-amine was treated with 1.5 mol % of each complex in thf-d_8 at 60 °C and the reactions were monitored regularly by ^1H NMR spectroscopy. The reaction was regioselective for the five-membered ring in all four experiments, producing 2-methyl-1-pyrroline as the sole product of reaction. The complexes with bis(pyrazolyl)methane ligands produced superior conversion rates and turnover numbers. The iridium(I) analogue **4**, in particular, reached full conversion in just over 2 h (Table 3). Significant improvement in the turnover rates was found at the somewhat higher reflux temperature (67 °C), with the iridium analogue **4** achieving full conversion in only 30 min and the rhodium analogue **3** reaching complete conversion in only 4 h.

The four complexes tested were further differentiated by the catalyst lifetime. For each of the catalysts studied, several reaction cycles were followed, where additional batches of substrate were added consecutively to the reaction mixture following complete conversion

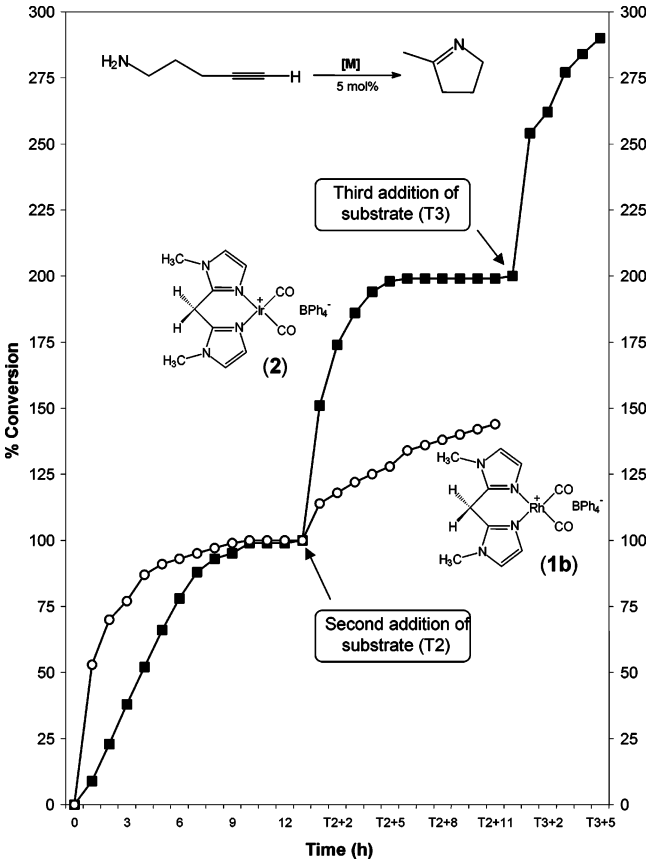

Figure 4. Reaction profiles of the $[Rh(bim)(CO)_2]^+[BPh_4]^-$ (**1a**) and $[Ir(bim)(CO)_2]^+[BPh_4]^-$ (**2**) catalyzed cyclization of 4-pentyn-1-amine with the batchwise addition of aliquots of substrate (5 mol % catalyst, tetrahydrofuran-d_8, 60 °C, second and third aliquots of substrate added at times T2 and T3, respectively).

of the initial substrate loading. These experiments clearly demonstrated that the iridium complexes were significantly more robust under the reaction conditions and continued to act as effective catalysts over several cycles, while the performances of the rhodium analogues were reduced on addition of new substrate (Figure 4).

Effects of Coligands and Counterions. The role of the CO ligands in the catalyzed reaction was investigated through the synthesis of a derivative of **1a**, where the CO ligands were substituted by PPh_3 to form $[Rh(bim)(PPh_3)_2]^+[BPh_4]^-$ (**1d**). The PPh_3 ligand has a more significant steric impact than CO, and the relative strengths of the metal−CO and metal−phosphine bonds as well as the relative labilities of the carbonyl and triphenylphosphine ligands may also influence the efficiency of the catalysis. The cyclization of 4-pentyn-1-amine with **1d** was significantly slower than with **1a** under identical conditions (Table 4). The coligands do have a significant impact on the reaction rate. This indicates either that the nature of the coligand affects the relative stability of reactive intermediates in the reaction pathway or that the initial coligand dissociation has a significant impact on the reaction rate.

The efficiency of hexafluorophosphate and tetrafluoroborate analogues $[Rh(bim)(CO)_2]^+[PF_6]^-$ (**1b**) and $[Rh(bim)(CO)_2]^+[BF_4]^-$ (**1c**) as catalysts was investigated to assess the potential influence of the counterion on the catalytic activity of the charged transition-metal

(28) Zuccaccia, C.; Macchioni, A.; Orabona, I.; Ruffo, F. *Organometallics* **1999**, *18*, 4367.

Table 4. Yield of 2-Methyl-1-pyrroline Obtained from the Rhodium(I)-Catalyzed Cyclization of 4-Pentyn-1-amine in Tetrahydrofuran-d_8 at 60 °C with a Variation of Coligand and Counterion

complex	conversn (%)	time (h)	N_t[a]
$[Rh(bim)(CO)_2]^+[BPh_4]^-$ (**1a**)[d]	100[b]	14	17
$[Rh(bim)(CO)_2]^+[PF_6]^-$ (**1b**)[e]	59	24	2[c]
$[Rh(bim)(CO)_2]^+[BF_4]^-$ (**1c**)[d]	18[b]	12	1[c]
	23	24	
$[Rh(bim)(PPh_3)_2]^+[BPh_4]^-$ (**1d**)[f]	63	24	2[c]

[a] Turnover number = (mol of product produced)/((mol of catalyst) h), typically calculated at time of 50% conversion. [b] Heating in the spectrometer magnet with spectra recorded every 10 min using an automated time course program. [c] Turnover calculated at 18% conversion. [d] Catalyst loading 1.5 mol %. [e] Catalyst loading 1.7 mol %. [f] Catalyst loading 1.4 mol %.

Table 5. Yield of 2-Methyl-1-pyrroline from the Rhodium- and Iridium-Catalyzed Cyclization of 4-Pentyn-1-amine with Catalysts 1a and 2−4 in the Presence of Excess 2-Methyl-1-pyrroline in Tetrahydrofuran-d_8 at 60 °C[a]

complex	amt of cat. (mol %)	time (h)	yield of 2-methyl-1-pyrroline (%)
$[Rh(bim)(CO)_2]^+[BPh_4]^-$ (**1a**)	1.6	15	36
$[Ir(bim)(CO)_2]^+[BPh_4]^-$ (**2**)	2	15	84
$[Rh(bpm)(CO)_2]^+[BPh_4]^-$ (**3**)	1.5	15	87
$[Ir(bpm)(CO)_2]^+[BPh_4]^-$ (**4**)	1.5	5	98

[a] One equivalent of 2-methyl-1-pyrroline was added to a solution containing 1 equiv of 4-pentyn-1-amine.

complex (Table 4).[29] The introduction of either the hexafluorophosphate or tetrafluoroborate counterion resulted in a decrease in catalyst activity compared to that of the complex with the tetraphenylborate counterion (Table 4). With $[Rh(bim)(CO)_2]^+[PF_6]^-$ **(1b)** as a catalyst, the rate of reaction decreased by approximately 40%. An even greater influence was evident for the reaction of 4-pentyn-1-amine with $[Rh(bim)(CO)_2]^+[BF_4]^-$ (**1c**), where only 23% conversion to the cyclized product was achieved after 24 h. The reduced activity with the smaller, more coordinating anions indicates that the nature of the counterion is important in determining the catalyst performance for this reaction.

Reaction Kinetics and Product Inhibition. The pyrroline product of the cyclization reaction contains a nitrogen atom that could itself behave as a donor, competing with the substrate for binding sites at the metal center. The impact of the product buildup on the reaction rate was examined by performing cyclization of the substrate 4-pentyn-1-amine in the presence of the reaction product 2-methyl-1-pyrroline using complexes **1a** and **2**−**4** as catalysts.

Approximately 1 equiv of 2-methyl-1-pyrroline was added to a solution containing 1 equiv of 4-pentyn-1-amine and the catalyst (∼1.5 mol %) in tetrahydrofuran-d_8. Reactions were performed at 60 °C and monitored by ^{1}H NMR spectroscopy (Table 5).

Comparison of the conversions presented in Table 5, obtained in the presence of excess product (2-methyl-1-pyrroline), with those in Table 3, which present the catalyzed cyclization under a standard set of conditions, demonstrates a significant inhibitory effect of the product on the catalytic activity. The inhibition is

(29) Analogous complexes synthesized using tetrakis(3,5-bis(trifluoromethyl)phenyl)borate as the counterion were not sufficiently stable to permit characterization.

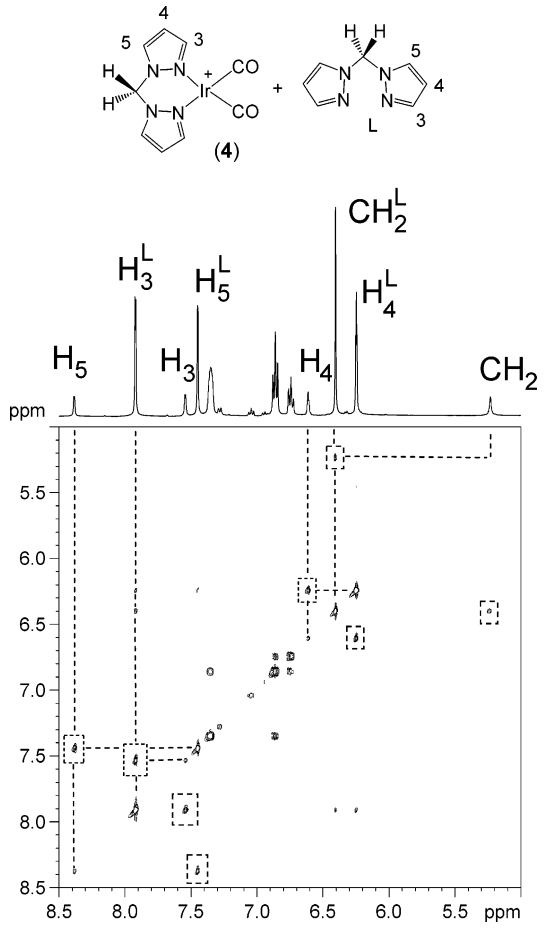

Figure 5. 2D EXSY spectrum (400 MHz, tetrahydrofuran-d_8, 210 K) of $[Ir(bpm)(CO)_2]^+[BPh_4]^-$ (**4**) in exchange with free bpm ligand (the cross-peaks due to exchange are marked with dashed squares).

particularly pronounced for the rhodium catalyst $[Rh(bim)(CO)_2]^+[BPh_4]^-$ **(1a)**. When using **1a** as a catalyst, 100% conversion was achieved after 14 h in the absence of any additional product and only 36% conversion was obtained after 15 h in the presence of excess 2-methyl-1-pyrroline.

Ligand Lability. N-donor ligands are, in general, more labile than those containing the more strongly binding phosphine or carbene donors. In solution, the bidentate N-donor ligands coordinated to the metal center underwent rapid exchange with added free ligand and 2D EXSY and variable-temperature NMR experiments were used to study the exchange. Qualitative data gave an indication of the relative rates of exchange of bim and bpm with the rhodium and iridium catalysts in solution. Typically, 1 equiv of the bidentate ligand was added to the complex in acetone-d_6 or tetrahydrofuran-d_8 in an NMR tube under nitrogen. The reactions occurred immediately at room temperature, and no heating was required to initiate the ligand exchange.

For $[Ir(bpm)(CO)_2]^+[BPh_4]^-$ (**4**) in the presence of excess free bpm ligand, the ^{1}H NMR spectrum exhibited very broad ligand resonances at room temperature indicative of rapid exchange between **4** and free bpm ligand. In addition to the usual NOESY-type cross-peaks between protons in the BPh_4^- counterion, the strongest peaks in the 2D EXSY spectrum (acquired at 210 K; Figure 5) are the series of cross-peaks arising from

exchange between the uncoordinated bpm ligand and the ligand bound to iridium. Similar ligand exchange was observed between $[Ir(bim)(CO)_2]^+[BPh_4]^-$ (**2**) and added free bim ligand. $[Rh(bim)(CO)_2]^+[BPh_4]^-$ (**1a**) and $[Rh(bpm)(CO)_2]^+[BPh_4]^-$ (**3**) also showed exchange with the corresponding free ligand. The rate of exchange was slowest for $[Rh(bim)(CO)_2]^+[BPh_4]^-$ (**1a**), with the ^1H NMR resonances for the free and coordinated ligand independently observed at room temperature.

In competitive ligand binding studies with rhodium complexes, there was no exchange between the ligands upon addition of approximately 1 equiv of bpm to $[Rh(bim)(CO)_2]^+[BPh_4]^-$ (**1a**). Conversely, the addition of bim to $[Rh(bpm)(CO)_2]^+[BPh_4]^-$ (**3**) resulted in complete displacement of the bpm ligand with bim, suggesting that the bidentate imidazole ligand binds more strongly to the rhodium center.

Conclusions

This paper explores characteristics of the cationic Ir(I) and Rh(I) complexes which catalyze intramolecular hydroamination of aminoalkynes. In terms of chemical robustness, the iridium complexes examined demonstrated much greater lifetimes than their rhodium analogues. The ligands were found to be labile, with the bis(pyrazolyl)methane ligand more labile than the bis(1-methylimidazol-2-yl)methane ligand. The complexes with the more labile bis(pyrazolyl)methane ligands produced superior conversion rates and turnover numbers. The most active catalyst of those studied was the Ir complex $[Ir(bpm)(CO)_2]^+[BPh_4]^-$ (**4**).

The nature of the counterion associated with the cationic catalysts does have a significant effect on the rate of the hydroamination reaction, and this indicates a strong anion/cation interaction in solution. The fact that these interionic interactions are clearly visible by NOE spectroscopy indicates that there is a long-lived association between the cations and anions (ion pairing) in the reaction mixture. This ion pairing could influence the formation of the active catalytic species and affect both access of the substrate to the reactive metal center as well as the charge distribution and electronic properties at the metal center.

Among the limited set of counterions examined, there is a trend toward increased reactivity with the bulkier, less coordinating anions. This trend suggests that catalytic activity may well be improved by further reducing the coordinating ability of the anions in solution. On the other hand, the stabilizing effect of suitable anions undoubtedly influences the chemical stability of the catalyst and, in practical terms, increased reactivity may have to be balanced against the convenience of handling a relatively stable catalyst system.

Experimental Section

All manipulations of metal complexes and air-sensitive reagents were carried out using standard Schlenk, high-vacuum, and glovebox techniques. Air-sensitive NMR samples were prepared in a nitrogen-filled glovebox with the solvent being vacuum-transferred into an NMR tube fitted with a concentric Teflon valve.

All organic starting materials were obtained from Aldrich Chemical Co. Inc. Rhodium(III) trichloride hydrate was obtained from Aldrich or Johnson Matthey and was used without further purification. Iridium(III) trichloride hydrate was obtained from Strem and used without further purification.

Tetracarbonyldichlorodirhodium, $[Rh_2(CO)_4Cl_2]$, was synthesized by the procedure described by McCleverty and Wilkinson.[30] $[Ir_2(COD)_2Cl_2]$ was prepared by the method of Herde.[31] The ligands bim[10] and bpm[20] were prepared by literature methods. Complexes **1**[10,21] and **4**[24] were also prepared by following literature methods.

4-Pentyn-1-amine was synthesized from 5-bromo-1-pentyne by reaction with liquid ammonia. Tetrahydrofuran and hexane were dried over sodium wire and distilled under nitrogen immediately prior to use from sodium benzophenone−ketyl. Methanol was distilled from magnesium turnings under nitrogen. Acetone was distilled from $CaSO_4$ under nitrogen. Deuterated solvents for NMR purposes were obtained from Merck and Cambridge Isotopes. Chloroform-*d* was used as supplied. Tetrahydrofuran-d_8 was dried over sodium/benzophenone and vacuum-distilled immediately prior to use. Acetone-d_6 was dried over molecular sieves and vacuum-distilled immediately prior to use.

^1H and ^{13}C NMR spectra were recorded on a Bruker DRX400 spectrometer at 400.13 and 100.62 MHz, respectively. ^1H and ^{13}C NMR chemical shifts (δ) were referenced to internal solvent resonances. All spectra were recorded at 300 K for characterization purposes unless otherwise stated and at 333 K for NMR-monitored catalytic reactions. Infrared spectra were recorded on a Perkin-Elmer 1600 Series FTIR spectrometer, the samples being recorded as KBr disks. Melting points were determined using a Gallenkamp apparatus and are uncorrected. Elemental analyses were carried out at the Campbell Microanalytical Laboratory, University of Otago, Otago, New Zealand.

Synthesis of (Bis(1-methylimidazol-2-yl)methane)dicarbonyliridium(I) Tetraphenylborate (2). Solutions of bis(1-methylimidazol-2-yl)methane (252 mg, 1.43 mmol) in methanol (5 mL) and sodium tetraphenylborate (548 mg, 1.6 mmol) in methanol (5 mL) were added to a solution of $[Ir(COD)Cl]_2$ (457 mg, 0.68 mmol) in methanol (20 mL) and hexane (5 mL) at room temperature. The reaction mixture was stirred for 2 h, degassed, and placed under an atmosphere of carbon monoxide gas for 3 days, during which time a pale yellow solid formed. The solid was isolated by filtration and washed with hexane and methanol. Recrystallization from acetone produced orange crystals of (bis(1-methylimidazol-2-yl)methane)dicarbonyliridium(I) tetraphenylborate (**2**; 895 mg, 89%). Mp: 190−193 °C dec.

Synthesis of (Bis(1-pyrazolyl)methane)dicarbonylrhodium(I) Tetraphenylborate (3). A solution of bis(1-pyrazolyl)methane (76 mg, 0.51 mmol) in methanol (5 mL) was added to a solution of $[Rh(CO)_2Cl]_2$ (100 mg, 0.26 mmol) in methanol (20 mL) at room temperature. The reaction mixture was stirred for 1 h, and an excess of sodium tetraphenylborate (150 mg) in methanol (5 mL) was added. The yellow solid that precipitated was filtered immediately, as the solution began to discolor, and washed with methanol. Recrystallization from acetone produced fine yellow crystals of (bis(1-pyrazolyl)-methane)dicarbonylrhodium(I) tetraphenylborate (**3**; 228 mg, 71%). Mp: 151−152 °C dec. ^1H NMR (400 MHz, tetrahydrofuran-d_8): δ 7.88 (d, 2H, *H5*), 7.36 (m, 10H, *H3* and *o-H*), 6.86 (t, 8H, *m-H*), 6.73 (t, 4H, *p-H*), 6.36 (t, 2H, *H4*), 5.25 (br(s), 2H, C*H*$_2$) ppm. $^{13}C\{^1H\}$ NMR (100 MHz, tetrahydrofuran-d_8): δ 183.4 (d, $^1J_{Rh-CO} = 70$ Hz, Rh−*C*O), 165.7−164.3 (m, B−*C*), 147.2 (*C5*), 137.1 (*o-C*), 135.7 (*C3*), 126.2 (*m-C*), 122.3 (*p-C*), 109.0 (*C4*), 63.2 (*C*H$_2$) ppm. IR (KBr): ν 2093 (Rh−CO), 2032 (Rh−CO) cm^{-1}. Anal. Found: C, 63.5; H, 4.7; N, 9.1. Calcd for $C_{33}H_{28}BN_4O_2Rh$: C, 63.3; H, 4.5; N, 8.9.

(30) McCleverty, J. A.; Wilkinson, G. *Inorg. Synth.* **1991**, *28*, 84.
(31) Herde, J. L.; Lambert, J. C.; Senoff, C. V. *Inorg. Synth.* **1974**, *15*, 18.

Synthesis of (Bis(1-methylimidazol-2-yl)methane)dicarbonylrhodium(I) Hexafluorophosphate, [Rh(bim)(CO)$_2$]$^+$[PF$_6$]$^-$ (1b). A solution of bis(1-methylimidazol-2-yl)methane (80 mg, 0.45 mmol) in methanol (5 mL) was added to a solution of [Rh(CO)$_2$Cl]$_2$ (88 mg, 0.22 mmol) in methanol (15 mL) at room temperature. The yellow precipitate that formed initially disappeared upon completion of ligand addition. The mixture was stirred for 30 min before adding an excess of potassium hexafluorophosphate (400 mg) in methanol (10 mL). The resulting precipitate was filtered and washed with methanol. (Bis(1-methylimidazol-2-yl)methane)dicarbonylrhodium(I) hexafluorophosphate (**1b**) was recrystallized from acetone as a dark pink solid (191 mg, 90%). Mp: 262 °C dec. Anal. Found: C, 27.6; H, 2.2; N, 11.4. Calcd for $C_{11}H_{12}F_6N_4O_2PRh$: C, 27.5; H, 2.5; N, 11.7. ^{1}H NMR (400 MHz, acetone-d_6): δ 7.55 (d, 2H, $^3J_{H5-H4}$ = 1.4 Hz, *H5*), 7.42 (d, 2H, *H4*), 4.63 (s, 2H, CH_2), 3.97 (s, 6H, N−CH_3) ppm. ^{13}C{^{1}H} NMR (100 MHz, acetone-d_6): δ 185.3 (d, $^1J_{Rh-CO}$ = 68.2 Hz, Rh−*C*O), 143.9 (*C2*), 130.9 (*C5*), 124.3 (*C4*), 34.8 (N-*C*H$_3$), 24.4 (*C*H$_2$) ppm. ^{31}P{^{1}H} NMR (162 MHz, acetone-d_6): −135 (sep, J_{P-F} = 708 Hz. *P*F$_6$) ppm. ^{19}F NMR (377 MHz, acetone-d_6): −67.5 (d, J_{F-P} = 708 Hz, PF$_6$) ppm. IR (KBr): ν 2084 (Rh−CO), 2026 (Rh−CO) cm^{-1}. MS (ES$^+$): *m*/*z* 335 (100%, [Rh(bim)(CO)$_2$]$^+$).

Synthesis of (Bis(1-methylimidazol-2-yl)methane)dicarbonylrhodium(I) Tetrafluoroborate, [Rh(bim)(CO)$_2$]$^+$[BF$_4$]$^-$ (1c). A solution of bis(1-methylimidazol-2-yl)methane (50 mg, 0.29 mmol) in methanol (5 mL) was added to a solution of [Rh(CO)$_2$Cl]$_2$ (50 mg, 0.13 mmol) in methanol (10 mL) at room temperature. The yellow precipitate that formed initially disappeared upon completion of ligand addition. The mixture was stirred for 1 h before an excess of sodium tetrafluoroborate (45 mg, 0.41 mmol) in methanol (10 mL) was added. The resulting precipitate was filtered and washed with methanol, affording (bis(1-methylimidazol-2-yl)methane)dicarbonylrhodium(I) tetrafluoroborate (**1c**) as a dark pink solid (78 mg, 71%). Mp: 268 °C dec. Anal. Found: C, 31.1; H, 2.5; N, 13.1. Calcd for $C_{11}H_{12}BF_4N_4O_2Rh$: C, 31.3; H, 2.9; N, 13.3. ^{1}H NMR (400 MHz, dimethylformamide-d_7): δ 7.62 (d, 2H, $^3J_{H5-H4}$ = 1.7 Hz, *H5*), 7.41 (d, 2H, *H4*), 4.70 (s, 2H, CH_2), 3.97 (s, 6H, N−CH_3) ppm. ^{13}C{^{1}H} NMR (100 MHz, dimethylformamide-d_7): δ 185.5 (d, $^1J_{Rh-CO}$ = 66.6 Hz, Rh−*C*O), 144.0 (*C2*), 130.9 (*C5*), 124.5 (*C4*), 34.5 (N−*C*H$_3$), 24.4 (*C*H$_2$) ppm. ^{11}B NMR (128 MHz, dimethylformamide-d_7): 1.73 (br s, *B*F$_4$) ppm. ^{19}F NMR (377 MHz, dimethylformamide-d_7): −146.3 (br s, B*F*$_4$) ppm. IR (KBr): ν 2080 (Rh−CO), 2025 (Rh−CO) cm^{-1}. MS (ES$^+$): *m*/*z* 335 (100%, [Rh(bim)(CO)$_2$]$^+$).

General Procedures for Monitoring Catalytic Reactions. Catalytic reactions were performed on a small scale in an NMR tube fitted with a concentric Teflon valve. Reactions were typically performed with 0.5 mmol of substrate and 1.5 mol % of complex in approximately 0.5 mL of solvent under nitrogen. The progress of the reaction was monitored by ^{1}H NMR at regular intervals. Reactions were carried out in tetrahydrofuran-d_8 at 60 °C.

The conversion of starting material to product was determined by integration of the product resonances relative to the substrate peaks in the ^{1}H NMR spectrum. A 100% conversion was taken to be the time where no remaining substrate peaks (<1%) were evident in the NMR. The turnover rate (N_t/h) was calculated in units of (mol of product)/((mol of catalyst) h) and was calculated at the point of 50% conversion of substrate to product.

Crystal Structure Determination. An approximately prismatic fragment was cut from a large red crystal, coated in oil, and sealed in a glass capillary. The crystal was then mounted on a Rigaku AFC7R diffractometer employing graphite-monochromated Cu Kα radiation generated from a rotating anode. Cell constants were obtained from a least-squares refinement against 25 reflections located between 67 and 77° 2θ. Data were collected at 294(2) K with ω−2θ scans to 135° 2θ. The intensities of 3 standard reflections measured every 150 reflections did not change significantly during the data collection. An empirical absorption correction based on azimuthal scans of 3 suitable reflections was applied to the data. The data were corrected for Lorentz and polarization effects. Processing and calculations were undertaken with TEXSAN.[32] The structure was solved in the space group $P2_1/c$ (No. 14) by direct methods with SIR97[33] and extended and refined with SHELXL-97.[34] Anisotropic thermal parameters were refined for the non-hydrogen atoms of the structure model, and a riding atom model was used for the hydrogen atoms.

Acknowledgment. We gratefully acknowledge technical assistance from Dr. Warren Shaw (University of Sydney) with the synthesis of [Rh(bpm)(CO)$_2$]$^+$[BPh$_4$]$^-$, Sarah Wren for assistance, and financial support from the Australian Research Council (ARC). We also wish to acknowledge Johnson Matthey for the generous loan of metal precursors.

Supporting Information Available: X-ray crystallographic data are available as CIF files. This material is available free of charge via the Internet at http://pubs.acs.org.

OM0343871

(32) teXsan for Windows: Single-Crystal Structure Analysis Software; Molecular Structure Corp., 3200 Research Forest Drive, The Woodlands, TX 77381, 1997−1998.

(33) Altomare, A.; Cascarano, M.; Giacovazzo, C.; Guagliardi, A. *J. Appl. Crystallogr.* **1993**, *26*, 343.

(34) Sheldrick, G. M. SHELXL97: Program for Crystal Structure Refinement; University of Göttingen, Göttingen, Germany, 1997.